

Improving the shear wave velocity structure beneath Bucharest (Romania) using ambient vibrations

Elena Florinela Manea,^{1,2,3} Clotire Michel,² Valerio Poggi,^{2,4} Donat Fäh,²
Mircea Radulian¹ and Florin Stefan Balan¹

¹National Institute for Earth Physics, Calugareni, 12, Magurele, Ilfov, Romania. E-mail: flory.manea88@gmail.com

²Swiss Seismological Service, Sonneggstrasse, 5, ETH Zürich, Zürich, Switzerland

³Faculty of Physics, University of Bucharest, Atomistilor, 405, Magurele, Ilfov, Romania

⁴Global Earthquake Model (GEM) Foundation, Via Ferrata 1, Pavia, Italy

Accepted 2016 August 9. Received 2016 August 4; in original form 2015 November 23

SUMMARY

Large earthquakes from the intermediate-depth Vrancea seismic zone are known to produce in Bucharest ground motion characterized by predominant long periods. This phenomenon has been interpreted as the combined effect of both seismic source properties and site response of the large sedimentary basin. The thickness of the unconsolidated Quaternary deposits beneath the city is more than 200 m, the total depth of sediments is more than 1000 m. Complex basin geometry and the low seismic wave velocities of the sediments are primarily responsible for the large amplification and long duration experienced during earthquakes. For a better understanding of the geological structure under Bucharest, a number of investigations using non-invasive methods have been carried out. With the goal to analyse and extract the polarization and dispersion characteristics of the surface waves, ambient vibrations and low-magnitude earthquakes have been investigated using single station and array techniques. Love and Rayleigh dispersion curves (including higher modes), Rayleigh waves ellipticity and *SH*-wave fundamental frequency of resonance (f_0^{SH}) have been inverted simultaneously to estimate the shear wave velocity structure under Bucharest down to a depth of about 8 km. Information from existing borehole logs was used as prior to reduce the non-uniqueness of the inversion and to constrain the shallow part of the velocity model (<300 m). In this study, we use data from a 35-km diameter array (the URS experiment) installed by the National Institute for Earth Physics and by the Karlsruhe Institute of Technology during 10 months in the period 2003–2004. The array consisted of 32 three-component seismological stations, deployed in the urban area of Bucharest and adjacent zones. The large size of the array and the broadband nature of the available sensors gave us the possibility to characterize the surface wave dispersion at very low frequencies (0.05–1 Hz) using frequency–wavenumber techniques. This is essential to explore and resolve the deeper portions of the basin. The horizontal to vertical spectral ratio (H/V) curves provide important additional information about the structure and are here characterized by two major peaks. The first is attributed to the fundamental frequency of the basin, while the second can be interpreted as a mixture of the second higher mode of Rayleigh waves and other types of waves such as *SH* waves. This hypothesis has been verified by comparing the H/V curves with the *SH*-wave transfer function from the retrieved velocity structure. We could also approximate the *SH* transfer function with H/V ratios of earthquake recordings, providing additional verification of the robustness of the proposed velocity model. The Cretaceous bedrock depth was then inverted at each URS station from the fundamental frequency of resonance and using this model. A 3-D geophysical model for Bucharest has been constructed based on the integration of the inverted velocity profiles and the available geological information using a geographic information system.

Key words: Fourier analysis; Spatial analysis; Earthquake ground motions; Surface waves and free oscillations; Site effects.

1 INTRODUCTION

Bucharest is one of the most exposed European capitals to the earthquake hazard. The major earthquakes affecting the city have their origin in the Vrancea region located at contact between East European plate and the Intra-Alpine and Moesic subplates. Vrancea is an intermediate-depth source with a high concentration of events in a well-defined volume (between 60 and 200 km depth), where two to three events with magnitude $M_w > 7.0$ are generated each century (Radulian *et al.* 2000). Although Bucharest is situated away (at about 150 km) from the source zone of Vrancea, the city experienced significant damage during these past earthquakes (Marmureanu *et al.* 2006).

Recent seismic site response or microzonation studies of the city pointed out the importance of the local geological structure together (or in connection) with the source properties and the regional propagation path (Moldoveanu *et al.* 2004; Cioflan *et al.* 2004, 2009; Cioflan 2006; Marmureanu *et al.* 2010). The remarkable thickness of the sedimentary deposits, reaching more than 8 km (Hauser *et al.* 2001; Raileanu *et al.* 2005), and the unconsolidated soft sediment cover (Mandrescu *et al.* 2004) are responsible for the generation of the large amplification (Lungu *et al.* 1999). Cioflan *et al.* (2004) compiled geological and geophysical data available in the literature for the Bucharest area and proposed a geological model of the sediment structure below the city down to about 2 km, including a model for the bedrock depth. Such model was subsequently tested using numerical simulation of ground motion in the Bucharest area. That study highlighted the importance of using a 3-D model in order to capture the complexity of the local seismic site response. The aim of the present study is therefore to propose an improved 3-D velocity model of Bucharest Metropolitan area to be used in future seismic microzonation.

The distribution of the shear wave velocity and the total thickness of the sediments are key parameters in the definition of the seismic response of sedimentary basins. Surface wave analysis of ambient vibration recordings represents a convenient way to obtain such information in a simple and cost effective way, if compared to traditional geophysical investigations (Lachet & Bard 1994; Fäh *et al.* 2001; Satoh *et al.* 2001). Although these techniques are mostly applied to the near-surface site characterization, applicability to large depths is only restrained by the lowermost resolvable frequency (that is mainly controlled by type of employed sensors, the presence or the lack of sufficient energy in the signal and the array size and geometry) and the fulfilment of the initial working assumptions over the measuring area (e.g. no lateral variations, isotropy and elasticity of the soil material). In this study, we used a 35 km aperture array (URS array) located in Bucharest and adjacent areas. This array is composed of 32 broad-band seismological stations with a minimum interstation distance of 500 m. Such configuration potentially allows us to resolve depths in the order of several kilometres. Moreover, the structure below the measuring area is assumed to be relatively homogenous, with a smooth surface topography and relatively flat layering.

Among the available ambient vibration techniques, in this study we use the horizontal-to-vertical (H/V) Fourier spectral ratios (Nogoshi & Igarashi 1971; Nakamura 1989) on single station recordings and the three-component frequency–wavenumber analysis (3C F-K; Fäh *et al.* 2008; Poggi & Fäh 2010) for the array processing. The former is useful to obtain estimates of the fundamental frequency of resonance (f_0^{SH}) of the site (Bonnefoy-Claudet *et al.* 2006a,b) and to characterize the local Rayleigh wave ellipticity (or polarization) function (Lachet & Bard 1994; Fäh *et al.* 2001, 2003;

Parolai *et al.* 2004), whose shape is strongly controlled by the presence of large seismic velocity contrasts at depth, particularly the bedrock (Bonnefoy-Claudet *et al.* 2006b). Complementary, three-component array analysis is essential to retrieve the multimodal dispersion characteristics of surface waves (Love and Rayleigh) contained in the ambient vibration wavefield. In addition, we apply the H/V method to a set of moderate magnitude earthquake data (10 events, $3.7 < M_w < 4.3$) recorded by URS array in 2003–2004. The transverse to vertical spectral ratios (T/V) for *S* waves were computed to serve as a proxy for the shape of the *SH* transfer function.

In the past, several seismological studies were performed in Bucharest using single stations (Bonjer *et al.* 1999; Grecu *et al.* 2007; Zaharia *et al.* 2008) and array recordings (Sèbe *et al.* 2009), however no tentative of joint inversion of these datasets was performed. Sèbe *et al.* (2009), for instance, retrieved the fundamental mode dispersion of Love waves from eight teleseismic events using a modified frequency–wave number analysis with non-uniform wave velocities; in the inversion, the bedrock location was fixed *a priori* using the available borehole data from Mandrescu *et al.* (2004, 2007). Combined inversion of multiple datasets can help reducing the non-uniqueness of such inversion problem by adding additional information for the calibration of seismic velocities and the location of the layer interfaces. We propose a velocity model for the Bucharest area constructed through joint inversion of the different surface-wave dispersion data (Love and Rayleigh, including fundamental and higher modes), the fundamental frequency of resonance of the site, the Rayleigh waves ellipticity and data available from existing boreholes. For the inversion we used the modified version of the neighbourhood algorithm (Sambridge 1999; Wathelet 2008). The results obtained from the inversion at the URS stations were interpolated to retrieve a 3-D geophysical model using a geographic information system (GIS; ArcGis).

2 GEOLOGICAL SETTING

Bucharest is located in the Moesian Platform of Romania, a sedimentary formation of Palaeozoic age. Above Cretaceous (Mesozoic) and Miocene (Tertiary) deposits (isobaths around 1400 m depth), a Pliocene (Tertiary) shallow-water deposit (about 700 m thick) was settled (Lungu *et al.* 1999; Mandrescu *et al.* 2008). The near-surface geology consists mainly of Quaternary alluvial deposits that were first identified and categorized by Liteanu (1951) and then referenced by different authors with minor changes (Grecu *et al.* 2003; Mandrescu *et al.* 2004, 2007; Moldoveanu *et al.* 2004; Ciugudean-Toma & Stefanescu 2006; Kienzle *et al.* 2006; Bala *et al.* 2008, 2009).

The Quaternary sequence is divided into seven main sedimentary units (beginning from surface to depth, Fig. 1):

(1) Layer 1: Anthropogenic backfill and soil, recent surface sediments, made up of vegetal soil and clayey sediments, with a thickness locally reaching 15 m.

(2) Layer 2: Upper sandy-clayey unit, represented by Loess Holocene deposits, sandy clays and sands. The thickness of this layer varies between 2 and 5 m in the Dambovită–Colentina inter-fluvial domain, 10–16 m in the northern and southern plains (Baneasa–Pantelimon and Cotroceni–Vacaresti) and 1 m in the river meadows.

(3) Layer 3: Colentina sand and gravel unit, contains gravels and sands (with large variations in grain size) and bearing the Colentina–aquifer. The thickness of this layer is between 1 and 20 m and is lacking in the western part of Bucharest.

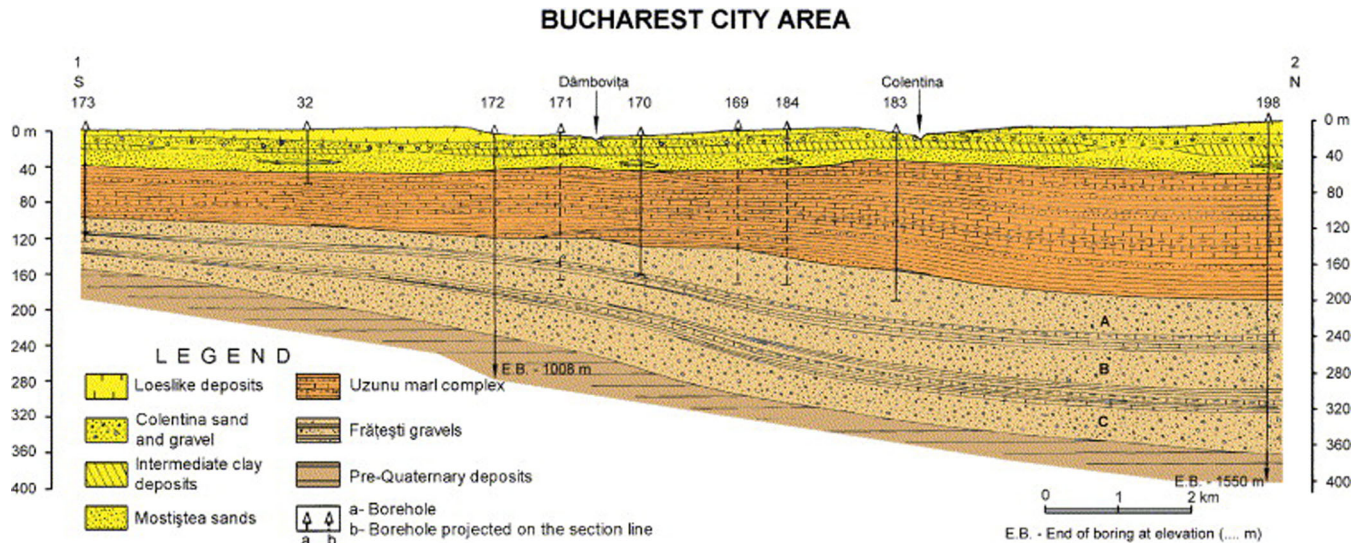


Figure 1. Lithological south–north cross-section (after Mandrescu *et al.* 2007). The anthropogenic backfill and soil are not shown in this section.

(4) Layer 4: Intermediate clay unit contains more than 80 per cent of hard consolidated clay and calcareous concretions with intercalated thin sand and silt lenses. The thickness of this layer varies between 0 and 25 m (south–north).

(5) Layer 5: Mostiștea sands unit, a confined water-bearing layer made up of fine grey sands with lenticular intercalation of clay. Its thickness varies from 10 to 15 m and is continuously present around Bucharest city.

(6) Layer 6: Lacustrine layer made of clays and silty clays, known as ‘Uzunul complex’, with small lenticular sandy layers and marl, most frequently situated at the top of this. The thickness is 10–60 m, and it can be found from about 60 m depth in the southern part of Bucharest to about 130 m depth in the north.

(7) Layer 7: Frățești is the lower gravel unit and bearing the Frățești aquifer. This layer consists in three thick sandy gravel layers (10–40 m each), separated by two marl or clay layers (each of 5–40 m thickness). This unit (total thickness 100–180 m) is present in the whole area of Bucharest and is dipping from the south (75 m depth) to the north (190 m depth).

3 DATA

During the 1977 earthquake ($M_w = 7.4$), strong site effects were revealed in Bucharest. Because of the impact of this event, many efforts were concentrated on the analysis of seismological data in order to develop a reliable velocity model to be used in the seismic microzonation of the city. Many projects have been developed in this direction, among which URS project (Ritter *et al.* 2005), BIGSEES project (Marmureanu, BIGSEES yearly report 2013) and ‘Impact of Vrancea earthquakes on the security of Bucharest city and other adjacent urban areas’ (Cioflan *et al.* 2007).

In the framework of BIGSEES national project (‘Bridging the Gap between Seismology and Earthquake Engineering: from the seismicity of Romania towards a refined implementation of seismic action EN1998-1 in earthquake resistant design of buildings’, 72/2012; Marmureanu, BIGSEES yearly report 2013), led by National Institute of Earth Physics (NIEP), a GIS database is under construction using all the available geological, geotechnical and geophysical information collected from previous projects or contracts performed by NIEP and publicly available. It contains in

particular velocity profiles obtained from boreholes using Seismic Cone Penetration Tests (SCPTU), Multi-Offset Vertical Seismic Profiling (MOVSP) and laboratory tests. The comparison between V_p and V_s estimates from the BIGSEES database and from other studies is presented in Tables 1 and 2.

In the framework of the cooperation between the National Institute of Earth Physics and the Karlsruhe Institute of Technology, 32 seismological stations equipped with broad-band velocity sensors were installed in Bucharest and adjacent areas (URS Experiment, Ritter *et al.* 2005; Fig. 2). The stations, synchronized by GPS, were recording from October 2003 to August 2004. The installed sensors comprise 22 STS-2 (120 s natural period), 5 Geotech KS2000 (100 s), 3 Guralp (40T and ESP, with 30 s period) and 2 Lennartz LE3D (5 s) seismometers. We selected recordings after instrumental response correction and a data quality control based on the power spectral density of the three components (north–south, east–west and Vertical), in the range 0.008–10 Hz.

Single station analysis of the ambient vibration recordings was performed on daily windows of 30 min over the entire available time span (10 months). For the array analysis, a large number of ambient vibration data sets with various durations (1 hr, 4 hr, 8 hr, 1 d, 5 d and 10 d) have been tested with the aim of retrieving a robust estimate of the dispersion curves.

During the period of the deployment, 4 seismic events with $M_w > 4$ and 48 seismic events with $M_w > 3$ occurred. In this study, 10 events with magnitude $M_w > 3.7$ and with a good signal to noise ratio are analysed (Table 3). These earthquakes all occurred in the Vrancea intermediate-depth area, at 140–160 km distance from Bucharest (Fig. 3).

4 PROCESSING

4.1 Single station analysis

Single-station seismic measurements were primarily used to assess the variability of the fundamental frequency of resonance of the S -wave (f_0^{SH}) over the different areas of the sedimentary basin. Therefore, H/V Fourier spectral ratios were computed on both ambient vibration and earthquake single station recordings. With some limitations, the H/V curves can also be used as a proxy to obtain

Table 1. Comparison of *P*-wave velocity (*V_p*) used in this study from BIGSEES project (Marmureanu 2013) and the ones proposed by Mandrescu *et al.* (2007) for the Quaternary sedimentary layers in Bucharest City area.

Layer no.	Upper limit of the layer (m)	<i>V_p</i> (m/s) (Marmureanu 2013)–this study	<i>V_p</i> (m/s) Mandrescu <i>et al.</i> (2007)
1. Backfill	0	230–670	200–400
2. Upper Clay	0.50–5.00	400–1246	485–750
3. Colentina Aquifer	5.00–12.00	541–1745	1200–1695
4. Intermediate clay	10.00–20.00	1000–1980	1650–2050
5. Mostistea aquifer	15.00–35.00	1486–1977	1200–1900
6. Lacustrine	35.00–50.00	1716–1975	1660–2000
7. Fratesti	100.00–180.00	1666–1820	1830–2300

Table 2. Comparison between shear wave velocities (*V_s*) used in this study from BIGSEES project (Marmureanu 2013) and the ones proposed by different authors for the Quaternary sedimentary layers in Bucharest City area.

Layer no.	Upper limit of the layer (m)	Marmureanu (2013)–this study	Lungu <i>et al.</i> (1999)	Bala <i>et al.</i> (2009)	Mandrescu <i>et al.</i> (2007)
1. Backfill	0	110–260	102	167	90–180
2. Upper Clay	0.50–5.00	140–330	102	244	210–320
3. Colentina Aquifer	5.00–12.00	243–383	333	270	300–350
4. Intermediate clay	10.00–20.00	278–441	236	327	320–450
5. Mostistea	15.00–35.00	313–413	271	340	350–400
6. Lacustrine	35.00–50.00	369–455	360	398	375–460
7. Fratesti	100.00–180.00	479–628	–	544	600–700

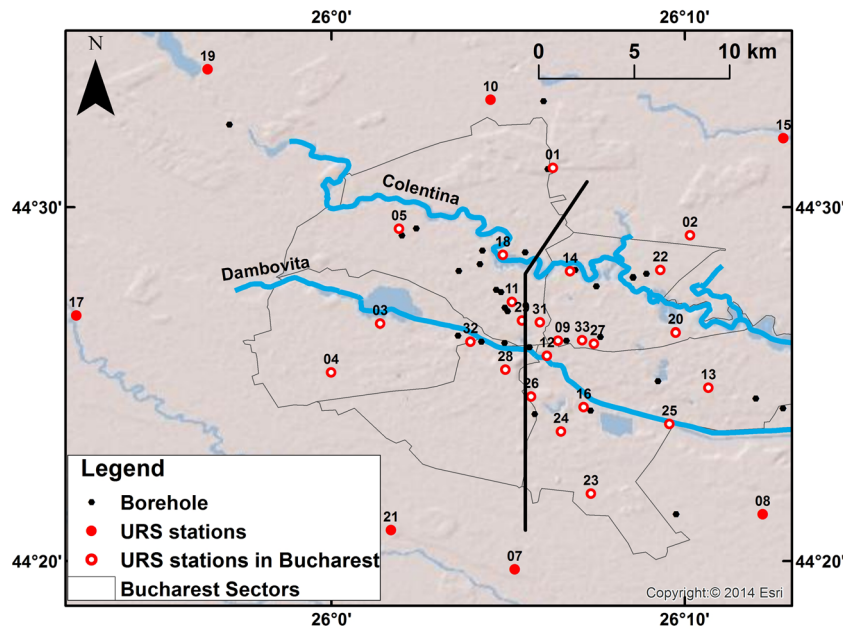


Figure 2. Location of the URS stations in Bucharest and adjacent areas. The black line represents the cross-section presented in Fig. 1.

Table 3. List of analysed earthquakes. For each earthquake, the origin date and time, location, depth, magnitude and the theoretical azimuth from the centre of the URS array are indicated.

Event ID	Date	Origin time (UTC)	Latitude (°)	Longitude (°)	Depth (km)	<i>M_w</i>	Theoretical backazimuth
95	2004/04/04	06:41:05	45.64	26.48	149.7	4.3	13.28
38	2004/02/07	11:58:22	45.65	26.62	143.5	4.3	17.28
77	2004/03/17	23:42:08	45.69	26.53	157.5	4.1	14.31
21	2004/01/21	05:49:11	45.52	26.46	117.7	4.1	13.96
97	2004/04/06	22:35:55	45.63	26.51	150.5	3.9	14.35
93	2004/04/02	03:21:04	45.73	26.67	142.1	3.8	17.96
115	2004/04/24	13:00:35	45.57	26.58	129.3	3.8	17.4
74	2004/03/14	05:26:41	45.73	26.74	127.5	3.8	19.93
44	2004/02/13	17:48:40	45.68	26.69	129.5	3.8	19.22
306	2003/11/02	18:16:32	45.7	26.83	96.1	3.7	22.6

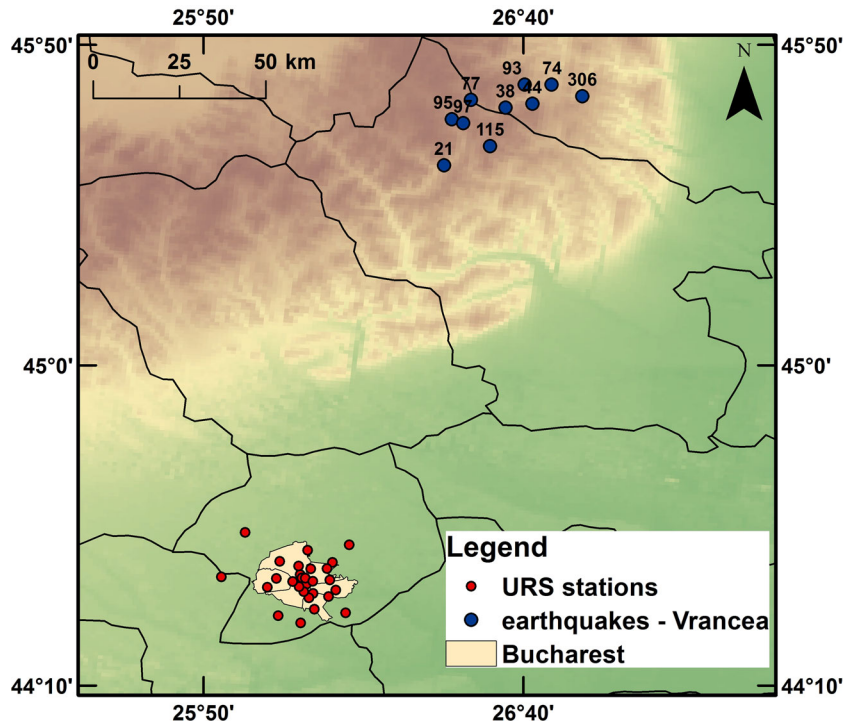


Figure 3. Location of the analysed earthquakes. The red circles are the URS stations located in Bucharest and the blue circles are the epicentres of the analysed earthquakes in Vrancea area.

the Rayleigh wave ellipticity function. In such a case, however, contribution of Love and body (especially S) waves may affect the estimate (Fäh *et al.* 2001), and assumptions have to be made (Fäh *et al.* 2003).

Standard H/V spectral ratios of the ambient vibration recordings were computed on daily windows of 30 min. Pre-processing consisted in removing any offset and linear trend (which typically affects broad-band recordings) by high-pass filtering. To perform better statistic on H/V, the signals were split in sub-windows of 150 s length and each sub-window tapered with a 10 per cent cosine taper before performing the spectral ratios. Spectra were subsequently smoothed using the Konno & Ohmachi (1998) algorithm with a bandwidth of 80, and the results from all windows averaged for each URS station separately. The latter is essential to obtain an estimate of the Rayleigh ellipticity function, particularly for the so-called ‘right flank’ of the H/V curve above f_0 (Fäh *et al.* 2001, 2003).

For earthquakes, the seismograms were rotated to their backazimuths to obtain the radial (R) and transverse (T) components. As in the case of ambient vibrations, earthquake data were pre-processed by removing the linear trend and by applying the same taper and smoothing type. The length of the S -waves window was 30 s and in order to obtain smooth curves until the fundamental frequency (0.1 Hz) of this site, zero-padding was applied until 100. The T/V ratio between the Fourier spectra of the transverse component and Fourier spectra of the vertical was computed to approximate the shape of the SH transfer function. The mean of T/V curves for all the earthquakes at each station was computed for S waves windows.

4.2 Array analysis

Ambient vibration array data were analysed using the three-component high-resolution frequency–wavenumber (3C F-K) anal-

ysis (Poggi & Fäh 2010), a modification of the method originally proposed by Capon (1969). This technique allows retrieving the multimodal dispersion characteristics of the Rayleigh (vertical and radial) and Love (transversal) waves by decomposing the wavefield into vertical, radial and transverse components of motion. Additionally, it can provide an estimate of the Rayleigh wave polarization function (ellipticity function) for the identified modes.

Two complementary array geometries were tested: one including all URS stations (the largest array of 35 km aperture) and one including only those stations located in the Bucharest area (a smaller array of 25 km aperture, Fig. 2). In both cases, a frequency range between 0.04 and 1 Hz was analysed, although the resolution of the smaller array does not allow to extract information below 0.1 Hz. The expected aliasing limits lie at about 1 Hz, but aliasing occurs actually below this value. For this processing, the time window is frequency dependent, the number of averaged frequencies is 5, the number of the stacked windows is 15 with an overlapping of 10 per cent and the number of maxima picked in k_x – k_y plane is 5. These values ensure in this case a good balance between the number of retrieved points and the accuracy in the dispersion plot.

The distribution of maxima in the slowness–frequency plane obtained for vertical and radial components on one side and transverse component on the other side is used to pick the Rayleigh and Love dispersion curves (fundamental and higher modes), respectively.

4.3 Inversion

The results from H/V, 3C F-K and borehole logging have been jointly inverted to obtain the 1-D velocity profile under the city. Inversion was performed using a global optimization approach based on a modified version of the neighbourhood algorithm (Wathelet *et al.* 2004; Wathelet 2008). This algorithm is an improvement of the original one proposed by Sambridge (1999). For a random initial set of

models (several thousands here), the misfit values were calculated and the next generation of models is located in the neighbourhood of the models with the lowest misfit values from the previous computation. In this way, the search is guided by the best models without neglecting the possible existence of better-fitting models further away.

The misfit function is the difference between the inverted parameters as: dispersion curves (Love and Rayleigh, fundamental and higher modes), the H/V curve as Rayleigh wave ellipticity, the *SH*-wave fundamental frequency of resonance (f_0^{SH}) and the corresponding values predicted from the model (determined from the solution of the forward model). A larger weight in the misfit function is applied to the dispersion information with respect to the other data. This is necessary to ensure a proper convergence of the solution.

In the inversion, only the right flank of the fundamental peak from the ellipticity curve (H/V curve) was used since the ellipticity can be identified best in this frequency range (Fäh *et al.* 2001; Hobiger *et al.* 2012). The ellipticity curve carries important information of the ground structure but due to the possible contribution of Love waves in the H/V curve, it can be biased around the trough and the peak frequencies (Hobiger *et al.* 2012). Therefore, we removed the part around the trough and the peak of the ellipticity and kept only the right flank. From the dispersion curves, only the part within the resolution bounds of the array was used (Wathelet *et al.* 2008). The extracted sections of dispersion curves are recursively compared and interpreted as fundamental or high-order modes (mode addressing) to end up with a final interpretation of the observations.

The resulting profiles are discrete representations of the elastic properties of the ground (V_p , V_s) and each profile is represented by a series of homogeneous horizontal layers. The parameter space has been defined using *a priori* information from the geology. In the upper part of the model (depth <300 m), the allowed velocity ranges are based on the borehole data of BIGSEES project (Marmureanu, BIGSEES yearly report 2013) (V_p and V_s , minimum and maximum values, see Tables 1 and 2). The density values are fixed *a priori* based on the available local information (borehole data (Marmureanu, BIGSEES yearly report 2013), refraction data from Hauser *et al.* 2001 and Raileanu *et al.* 2005). For the deeper part, the model was divided in six layers in concordance with the data from geology. The five layers until Cretaceous bed are present in all the area and

become thicker from the south to the north (Mandrescu *et al.* 2008). Because no information exists about the thickness of these layers, large variations are allowed in the inversion. The velocity below the interface with the bedrock (sixth layer) is constrained using the V_p , V_s , density and depth values from refraction data obtained by Hauser *et al.* (2001) and Raileanu *et al.* (2005).

Several constraints are added to drive the inversion to realistic models only (Wathelet 2008): the velocity is assumed to increase with depth (except in the upper part controlled by the borehole data) and the Poisson ratio is kept between 0.2–0.4 in the deep part of the model and in the range 0.2–0.47 for the upper layers, where higher V_p/V_s ratios due to the presence of aquifers were confirmed by borehole data. These assumptions are checked *a posteriori*: if the retrieved models reproduce the observations, one does not look for more complex models.

5 RESULTS

5.1 Single station analysis

The H/V Fourier spectral ratio of ambient vibrations was computed for each URS station in order to identify the fundamental resonance frequency (f_0) of the site and its Rayleigh ellipticity curve. The consistency of the H/V curves over the entire array suggests that there are no significant lateral variations within the subsoil of the city. Two predominant peaks can be seen with relatively low amplitudes that may show the absence of large impedance contrasts (Fig. 4). The fundamental peak (f_0), between 0.14 and 0.3 Hz, is attributed to the geophysical bedrock, interpreted as the interface between Tertiary and Cretaceous (Mesozoic) geological units, whose distribution confirms that the bedrock is dipping to the north at about 1.4 km depth (Greco *et al.* 2003; Fig. 5). The second peak, that is not well defined in the range 0.6–0.9 Hz (Bonjer *et al.* 1999; Greco *et al.* 2007; Zaharia *et al.* 2008), is correlated in the literature with the base of the Quaternary (Zaharia *et al.* 2008) and was attributed to the engineering bedrock (Bala 2014). At higher frequencies, the curves are particularly flat and do not exhibit shallow resonances in general.

The T/V ratios for the *S*-wave windows of earthquakes show a slightly different pattern (Fig. 6). The fundamental frequency is not

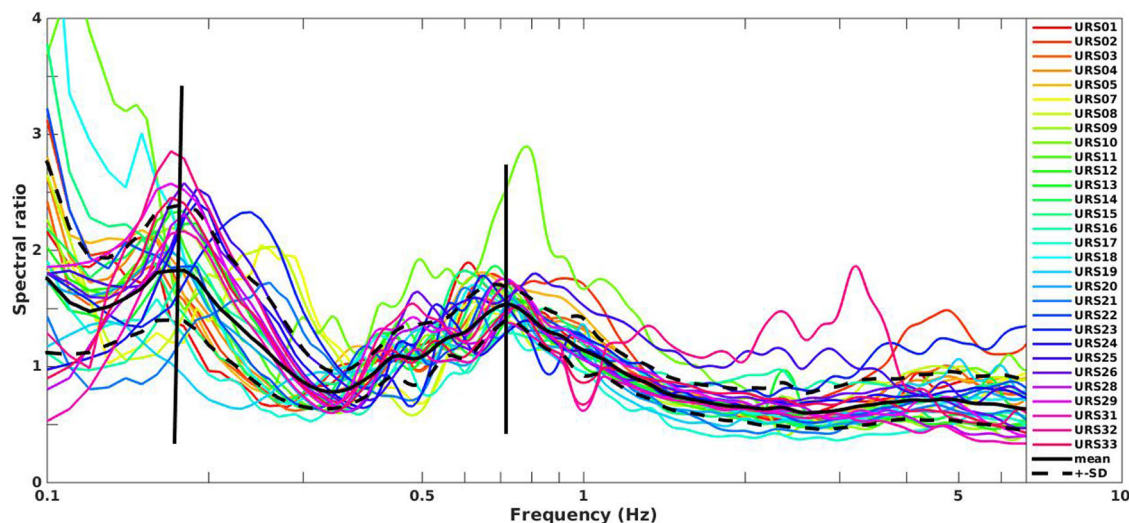


Figure 4. H/V spectral ratios of ambient vibrations at each URS station in Bucharest. The mean and standard deviation are represented in black. The two identified peaks are designated with a vertical black line.

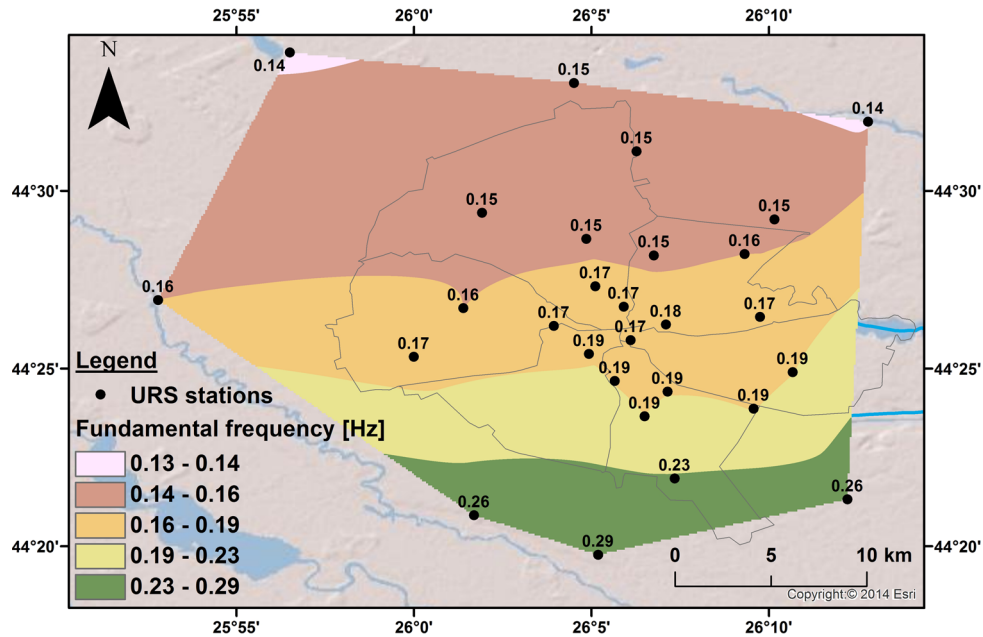


Figure 5. Variation of fundamental frequencies (f_0) over the entire city.

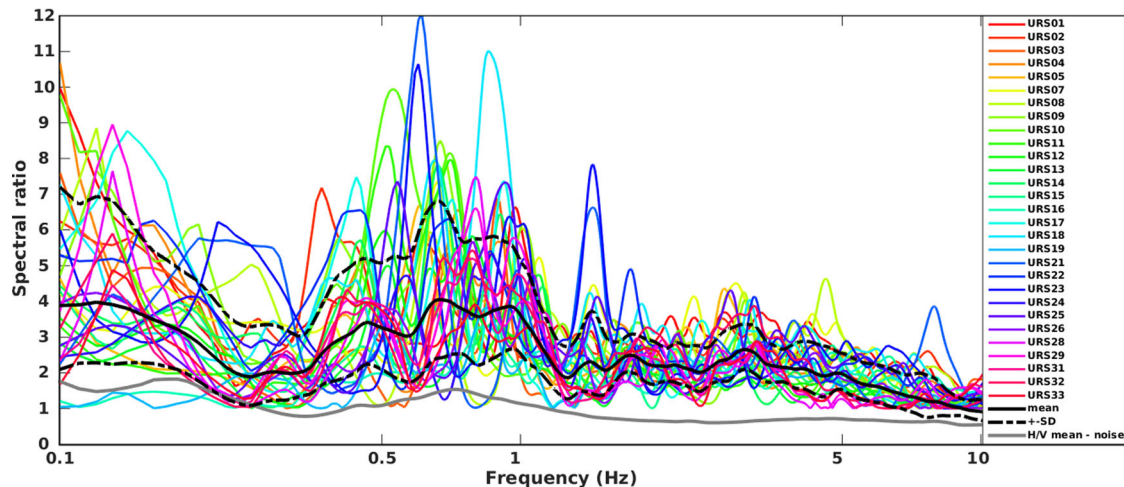


Figure 6. Mean T/V ratio from 10 earthquakes at each URS station in Bucharest. The black lines are the T/V mean curve and its standard deviation and the grey line is the H/V mean curve obtained from noise.

clearly visible due to the too short data windows. The variation of T/V ratio across the array is due to the change in the geological structure. Several peaks in the range 0.4 to 1 Hz are observed, with larger amplitudes than in the H/V ratios of ambient vibrations. Their interpretation is done in the section related to the 1-D inversion. The similarity of the T/V ratio for the central stations (URS28, URS31, URS32 and URS33) confirms that the geological structure under the centre of Bucharest is rather uniform (Fig. 6).

5.2 Array analysis

The 3C F-K analysis of ambient vibrations was used in order to retrieve information about the propagation of Love and Rayleigh waves (dispersion and ellipticity). The complete distribution of maxima around the fundamental modes in the slowness–frequency plane was used to estimate the mean and standard deviation of the dispersion curves, whereas the higher modes were peaked manu-

ally due to higher uncertainties. An example is shown in Fig. 7 for the transverse component and in Fig. 8 for the radial and vertical components, using the large array and 5 hr of recordings. The array limits are also displayed and show that the Rayleigh and Love dispersion curves can be retrieved with confidence between 0.06 and 1 Hz and 0.1 and 1 Hz, respectively. The retrieved dispersion curves for small and large arrays within their respective array limits have been merged. They show a strong velocity decrease between 0.07 and 0.25 Hz from 3500 down to 700 m s⁻¹. This drop corresponds most probably to the interface between the Cretaceous (Mesozoic) bedrock and the Tertiary and Quaternary sedimentary cover. The large aperture of the array allows to fully constrain this interface, which is rarely the case for classical applications, where the retrieved dispersion stops in its descending part (e.g. Michel *et al.* 2014). The interpretation of the Love and Rayleigh dispersion curves are presented in Fig. 9. We attribute the mean dispersion curves for Love and Rayleigh waves as being characteristic for the central structure of the array, though it corresponds to an average

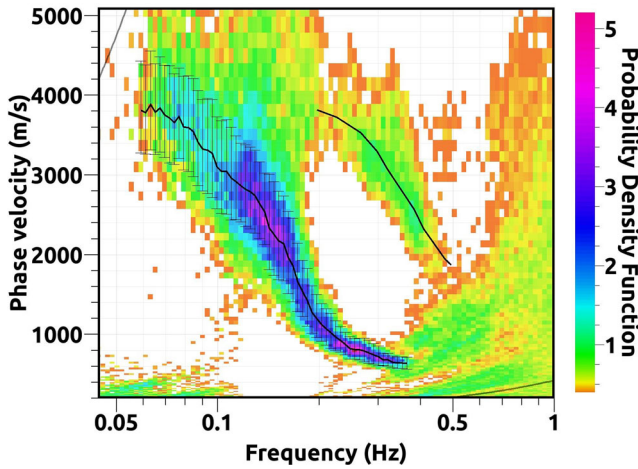


Figure 7. Density distribution of the surface waves signal of the transverse component, obtained using 3C F-K analysis for URS array. The black lines are the picked dispersion curves, the black bars are the standard deviations and the grey lines are the resolution and aliasing bounds of the array.

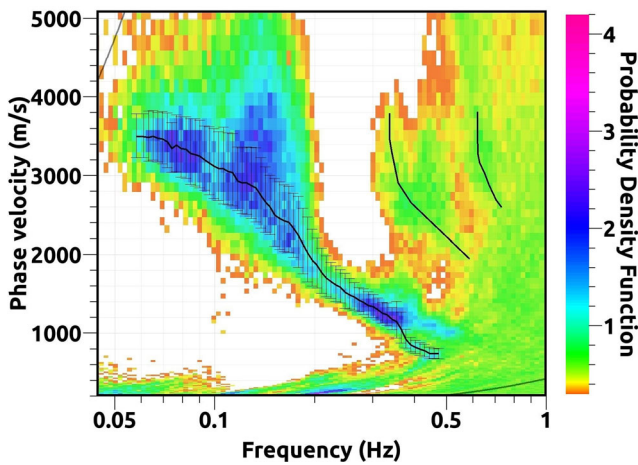


Figure 8. Density distribution of the surface waves signal of the radial and vertical components, obtained using 3C F-K analysis for URS array. The black lines are the picked dispersion curves, the black bars are the standard deviations and the grey lines are the resolution and aliasing bounds of the array.

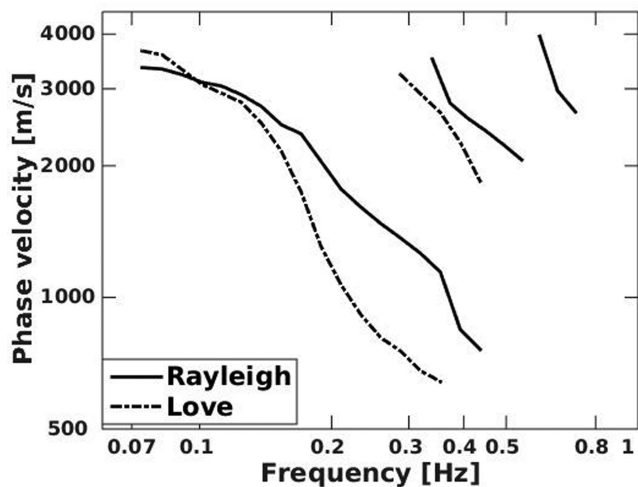


Figure 9. Final interpretation of the Rayleigh and Love dispersion curves for URS array using the 3C F-K analysis.

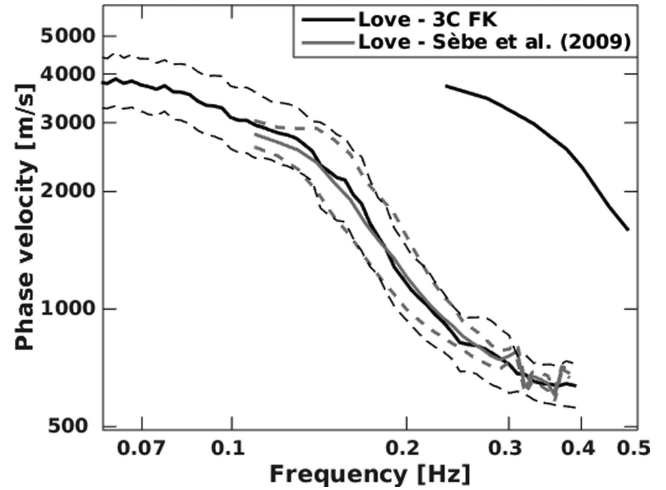


Figure 10. Comparison between the Love dispersion curves obtained from 3C F-K analysis and the dispersion curves from Sèbe *et al.* (2009). The dashed lines are the standard deviations of the dispersion curves.

over a large volume below the array. A large scatter is noticed around 0.1–0.2 Hz, as well as between 0.4 and 0.5 Hz that could only be explained after interpreting the inversion results. The mode addressing is also uncertain at this point and is solved during the inversion phase.

The comparison of the Love dispersion curves obtained using the 3C F-K analysis of ambient vibrations and the ones proposed by Sèbe *et al.* (2009), obtained using teleseismic events (Fig. 10), shows a good match between 0.1 and 0.4 Hz. Using the 3C F-K analysis of ambient vibrations, we could extend the frequency range of estimation between 0.04–0.7 Hz and, in addition, retrieve the dispersion curves of Rayleigh fundamental mode and higher modes of Love and Rayleigh waves. Sèbe *et al.* (2009) confirms the variability of the dispersion curves from north to south in Bucharest, represented as the uncertainty in Fig. 10. In our study, the phase velocities of Rayleigh waves are better seen from the radial than from the vertical component. The former component has more energy at high frequency and therefore at the higher modes. We verified that the distribution of Rayleigh wave sources was homogeneous so that no bias is expected between fundamental and higher modes. Other authors already reported that the radial component may provide segments of Rayleigh wave dispersion curves for modes that are not visible on the vertical component (Fäh *et al.* 2008; Poggi & Fäh 2010; Michel *et al.* 2014).

The Rayleigh wave ellipticity computed using 3C F-K is compared to the H/V mean curve in Fig. 11. As a result, the H/V curve obtained from ambient vibrations describes well the Rayleigh wave ellipticity except around the peak at 0.6 Hz where its amplitude is higher, indicating the contribution of other types of waves (Love, body waves).

5.3 Retrieval of the 1-D regional velocity profile

The surface wave dispersion curves (Love and Rayleigh, fundamental and higher modes), the *SH*-wave fundamental frequency of resonance (f_0^{SH}) and Rayleigh ellipticity were inverted to estimate the 1-D regional velocity profile. It should be reminded that the upper part of the profile, and therefore the higher frequencies (above 1 Hz) are constrained through the borehole data.

The hypothesis of attributing the three curves to the fundamental, first and second higher modes, was discarded after a first round

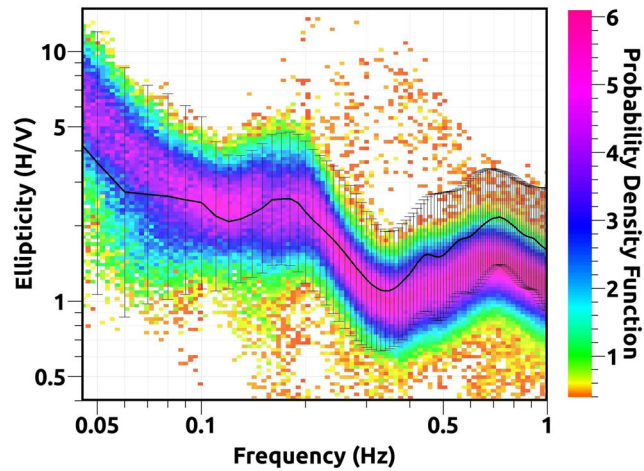


Figure 11. Density distribution of the surface waves signal of ellipticity of Rayleigh waves, obtained using 3C F-K analysis for URS array. It is compared with the H/V mean curve for Bucharest (black line) and its standard deviation (black bars).

of computation, since no model could reproduce these data. The higher modes have therefore been addressed as the second and third higher modes, which turned out to match with simple models. The inversion for the regional velocity profile is presented in Fig. 12. The computed parameters for the inverted models are in agreement with the observed ones, except the right flank of Rayleigh ellipticity curve. This misfit can be due to the contribution of other types of waves (Love, body waves) in the H/V curve.

The velocity values in the 6th layer obtained from refraction ($V_p = 5400 \text{ m s}^{-1}$, $V_s = 3000 \text{ m s}^{-1}$; Raileanu *et al.* 2005) and the retrieved shear wave velocity from inversions ($V_p = 5227 \text{ m s}^{-1}$ and $V_s = 2820 \text{ m s}^{-1}$) are in good agreement. The lowest interface representing the interface with the crystalline basement is necessary to reproduce the increasing velocity in the dispersion curve below 0.14 Hz. Therefore, the depth of the final model is around 8 km with a particularly good constrain down to the early Devonian (sixth layer) by the surface waves properties.

For this 1-D velocity structure, we computed the phase velocity of Rayleigh waves in order to understand the scattered energy observed in the density distribution of the surface waves signal on the radial and vertical components. Fig. 13 shows that both uncertain regions around 0.2 and 0.4 Hz correspond to a mode osculation of the

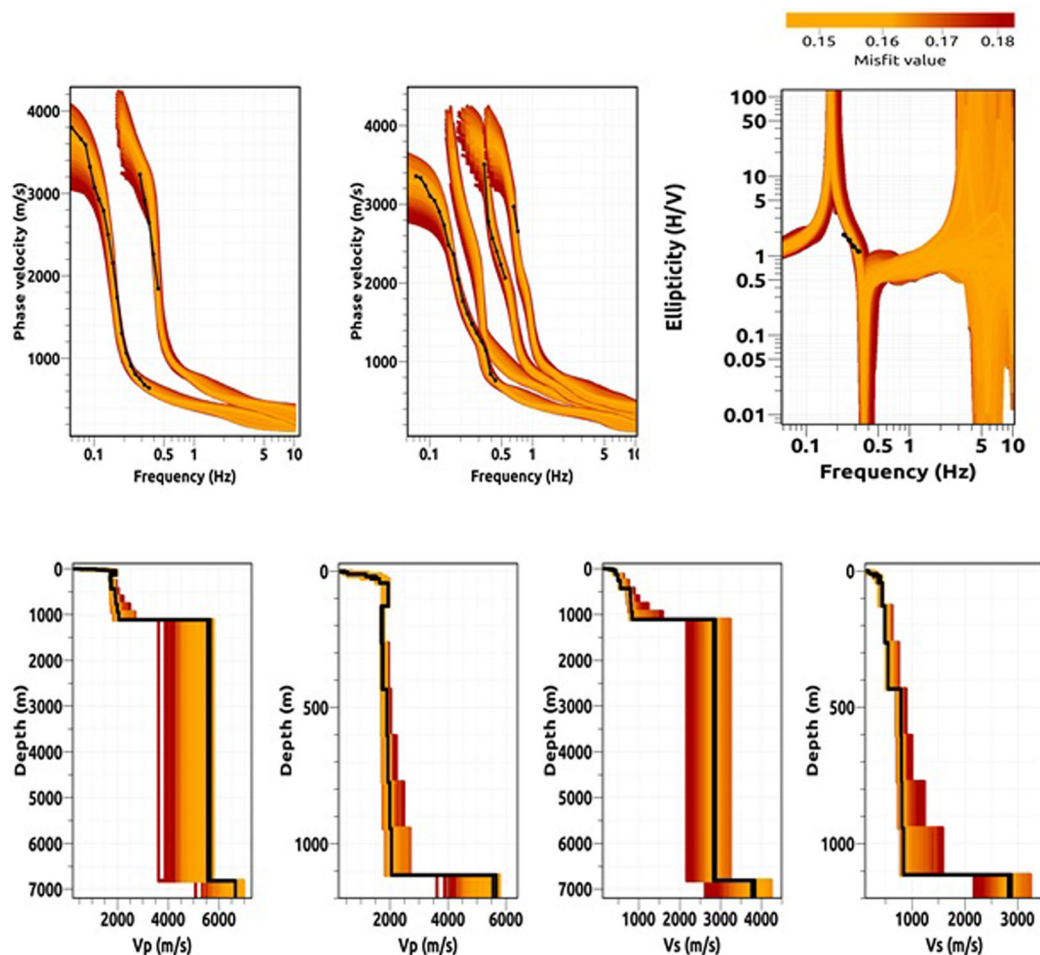


Figure 12. Combined inversion of dispersion curves (three modes of Rayleigh waves, two modes of Love waves) and right flank of the ellipticity of Rayleigh waves into velocity. The black dotted lines indicate the observed properties, whereas the background lines indicate the inverted properties. The scale, denoting the misfit value, is consistent across the different plots. The black line represents the best model. The upper part of the velocity model and therefore the frequencies above 1 Hz are constrained *a priori* using borehole data.

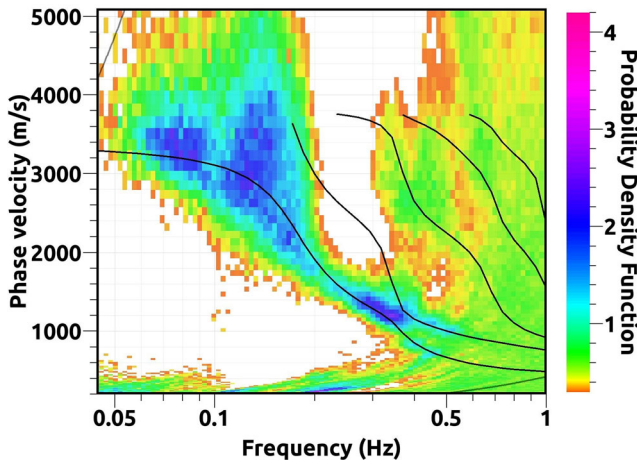


Figure 13. Density distribution of the surface waves signal of the radial and vertical components, obtained using the 3C F-K analysis for URS array. The black lines are the dispersion curves computed from the regional 1-D velocity model.

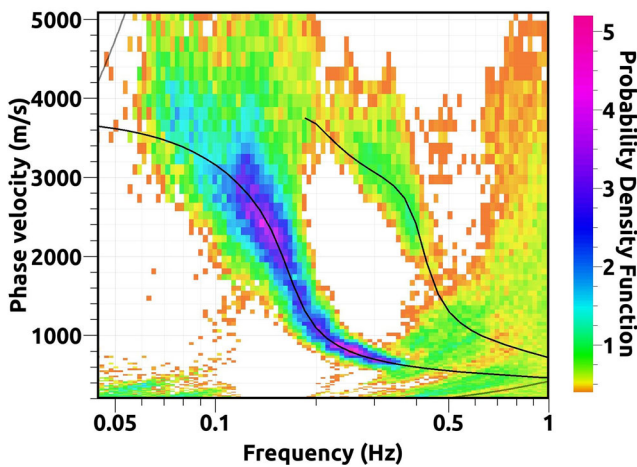


Figure 14. Density distribution of the surface waves signal of the transversal component, obtained using the 3C F-K analysis for URS array. The black lines are the dispersion curves computed from the regional 1-D velocity model.

fundamental and the first higher modes (Fig. 9). The phase velocity of Love waves shows a good match with the observations (Fig. 14).

The comparison between the retrieved velocity profile and the model proposed by Marmureanu *et al.* (2010) from numerical simulation is made in Fig. 15. The model of Marmureanu *et al.* (2010) does not show any impedance contrast at the interface between Tertiary and Cretaceous (Mesozoic) units. Moreover, it overestimates the shear wave velocity above this interface and underestimates the velocity in the bedrock. This model does not explain the observed dispersion curves neither the observed fundamental frequency.

The 1-D *SH* transfer function was calculated in order to retrieve the amplification of the site using the obtained model and the attenuation factor model (*Q*) proposed by Cioflan *et al.* (2009). First of all, its shape matches well with the T/V ratios from *S*-wave windows of earthquakes above 0.5 Hz (Fig. 16) showing that they are in this case a proxy for the shape of the amplification due to *SH* waves. The amplitude is in accordance as well but the T/V ratios are not related to an absolute reference rock and are largely controlled by complex interactions of the *P-SV* wavefield, which are difficult to quantify in practice. The fundamental peak at 0.2 Hz is not matching but is very

uncertain for the earthquake recordings: since 30 s windows have been used, a maximum of 6 cycles of the fundamental frequency is considered and most of the used events were too small and/or too deep to excite this mode.

Moreover, the second peak observed in the H/V curves (0.6–1 Hz) is not reproduced by the fundamental Rayleigh wave ellipticity of the retrieved 1-D model but it could be explained as a combination of the second higher mode of Rayleigh and other types of waves (Love, body waves). The comparison between the H/V curves and the *SH* transfer function shows that this peak could be due to the *SH* contribution in the H/V ratios of ambient vibrations (Fig. 16). The double peak observed in this transfer function corresponds indeed well with the unclear peak, sometimes double, observed in the H/V curves. This peak is due to the interface between the Quaternary and Neogene layers but its complexity is explained by the *SH* transfer function of the whole profile.

6 3-D VELOCITY MODEL

In order to retrieve a 3-D velocity model, we first developed velocity profiles for each URS stations and then interpolated the layers using a GIS.

The velocity profiles under each URS stations were made up using the information from the nearest boreholes (V_p , V_s values; Marmureanu, BIGSEES yearly report 2013) for the upper part of the model. In some cases, the identification of the depth of the different layers from borehole data was not unique and the results obtained by Mandrescu *et al.* (2007) were adopted. For the lower part of the model under each URS station, the Tertiary layers were divided into five equally spaced layers down to the Cretaceous bedrock, as for the regional model. The velocity from the retrieved regional model is assumed to remain the same in these layers (only the depth changes), which could however be biased since the compaction level of the sediments due to varying depth may influence the seismic velocity. In this way, we assume that in a deeper basin all the layers until sixth layer (early Devonian layer) are proportionally thicker, which comes from the observation of Fig. 1. The thickness of the sixth layer remains identical over the city and was constrained using the refraction data obtained by Hauser *et al.* (2001) and Raileanu *et al.* (2005).

The bedrock depth alone is then inverted with respect to the fundamental resonance frequency from the H/V curve. A similar approach has been successfully applied by Poggi *et al.* (2012). In this way, a good constrain of the bedrock depth was obtained and its variability in Bucharest can be seen in Fig. 17. The comparison of the bedrock depth with three deep boreholes (from Mandrescu *et al.* 2008) shows that the basement of the model is matching with the geological bedrock. The variation of the bedrock depth as a function of the fundamental frequency is presented in Fig. 18. The results were adjusted using a log-linear regression that can be used in future studies in the area if further single stations recordings are acquired:

$$\log(D) = -\log(f_0) + 5.2302, \quad (1)$$

where D is the bedrock depth and f_0 is the fundamental frequency. It can be rewritten as

$$D = \frac{747}{4f_0}, \quad (2)$$

with a traveltime average shear wave velocity over the entire sediment column of 747 m s^{-1} .

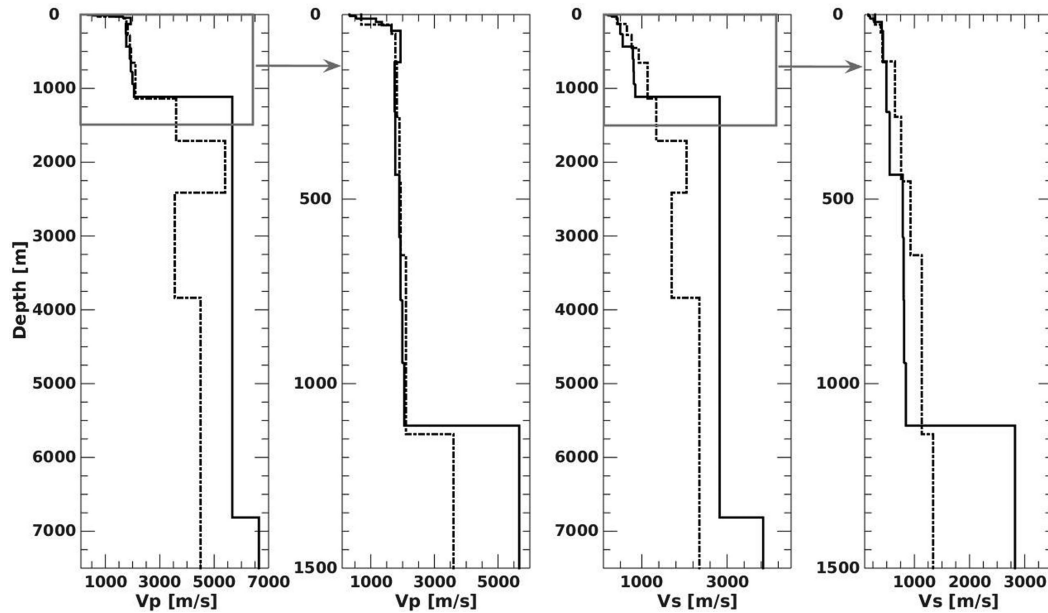


Figure 15. Comparison between the regional 1-D velocity model (solid line) and the model of Marmureanu *et al.* (2010) (dashed line).

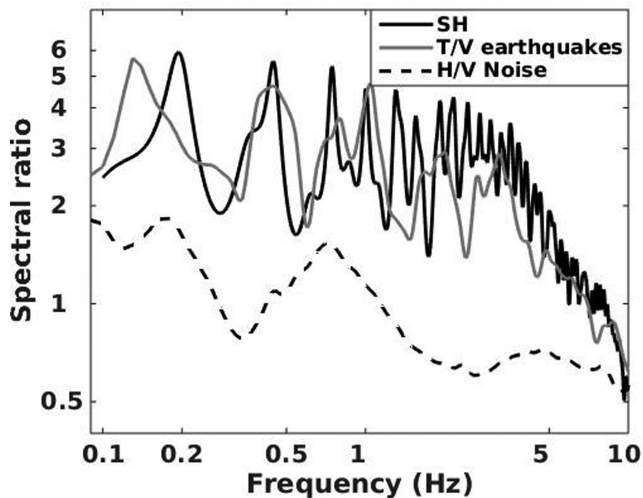


Figure 16. Comparison between the H/V ratios from ambient vibrations, T/V ratios from earthquakes and the *SH* transfer function of the regional 1-D velocity model.

In order to interpolate these results between the URS stations to retrieve a 3-D model, we used a GIS (ArcGIS tool (<https://www.arcgis.com/home/index.html>)). The depth of each layer was calculated from the digital elevation model at each URS station and was spatially interpolated to have its variation in Bucharest, using the Natural Neighbour method. This method is based on Voronoi cells using a discrete set of spatial points that are not necessary regularly distributed.

The final 3-D geophysical structure under Bucharest, showing the distribution of the main layers in depth (the bottom), is displayed in Fig. 19. The main feature that can be observed for all these layers is that they are dipping from the south to the north of the area in accordance with f_0 , as also shown by the north–south cross-section presented in Fig. 20.

7 DISCUSSION

We analysed the properties of surface waves in the city of Bucharest from ambient vibration recordings from a large array of broad-band sensors. This technique allowed us to investigate surface wave dispersion curves down to 0.06 Hz, corresponding to several kilometres depth. This could be achieved due to the relatively simple geometry of the basin, the very large URS array and the presence of sufficient amount of energy at these frequencies. The retrieved velocity model explains well the observed dispersion curves. The first higher mode of Rayleigh waves was generally not excited but mode oscillations are clearly seen on the FK plot. On the contrary, the interpretation of the H/V curve is more difficult. The retrieved model shows two singularities at the peak and at the trough of the ellipticity function, although the H/V curve is smoother. Its amplitude is also hardly matching, indicating a combination of Rayleigh waves with other types of waves (Love, body waves) in the H/V or a mixing of modes. The second peak at 0.6 Hz in the H/V curve is not observed on the fundamental ellipticity curve from the retrieved model but the results indicate that it can be interpreted as a mixture between the second higher mode of Rayleigh waves and *SH* waves. We also found out that the shape of the *SH* transfer function was well matching with the H/V from earthquake recordings in this case, which further validates the retrieved model.

The Bucharest basin area is therefore an excellent benchmark to understand the composition of the wavefield of ambient vibrations and earthquake recordings.

Another issue is related to the relevance of retrieving the full velocity profile (down to the basement) for hazard analysis. It has been observed that the damage to large structures in Bucharest in the past was due to a peak at 0.6 Hz in the response spectra of recorded ground motion (Grecu *et al.* 2003). We showed that this peak could be correctly explained only by understanding the whole velocity profile. It is therefore critical in microzonation studies to model the sub-surface at least down to the geophysical basement, corresponding to the observed fundamental peak in the H/V curve. Even if this interface separates what could be defined in terms of geology by rock layers, it plays a major role in the site response and therefore in the hazard analysis.

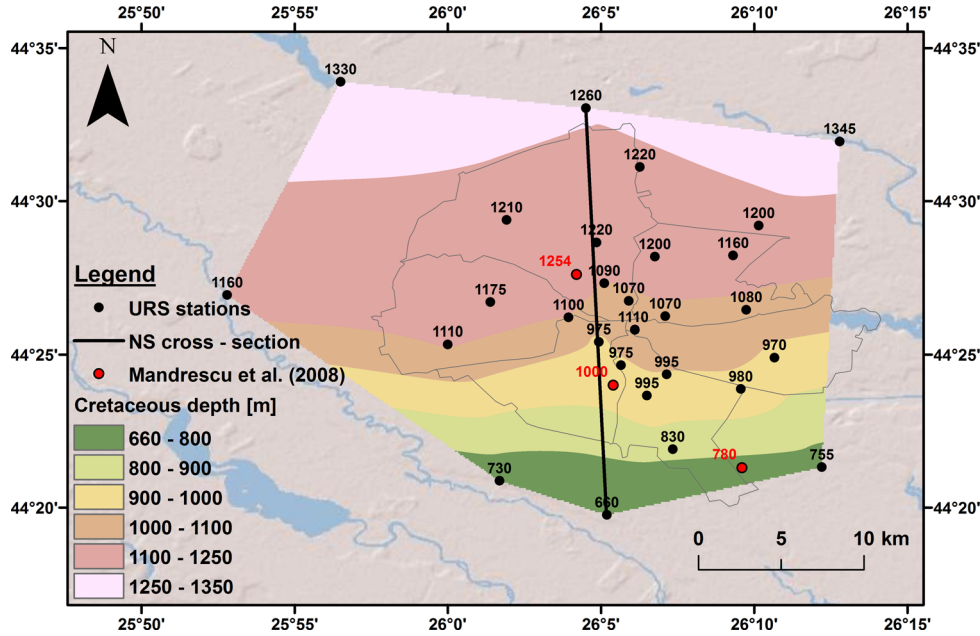


Figure 17. Bedrock depth obtained from the inversion of the fundamental frequency (see Fig. 5) and its comparison with the geological bedrock proposed by Mandrescu *et al.* 2008 (red points) under Bucharest. The black points are the computed depths [m].

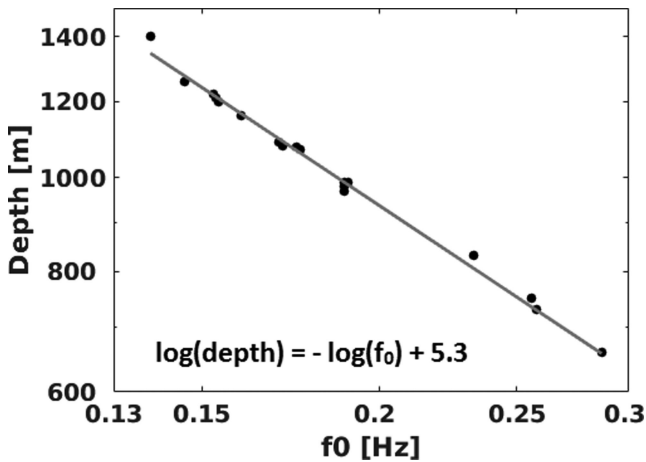


Figure 18. Variation of the bedrock depth as a function of the fundamental frequency and linear regression (grey line).

8 CONCLUSIONS

In this study, we performed a step forward toward in the understanding of earthquake effects in the city of Bucharest.

By improving the mapping the local geological and geophysical structure over the city area, we can better understand the seismic ground motion and its amplification. In order to construct a 3-D model for this city, non-invasive methods were applied: H/V spectral ratios of ambient vibrations and three-component array analysis of ambient vibrations. These methods, originally developed for near-surface applications, were successfully applied here to retrieve information on the deep structure (until 8 km depth) using a large aperture array of broad-band sensors.

The consistence of the H/V curves over the entire array suggests that there are no significant lateral variations within the subsoil of the city. The fundamental peak, between 0.14 and 0.3 Hz, is attributed to the geophysical bedrock, interpreted as the interface between

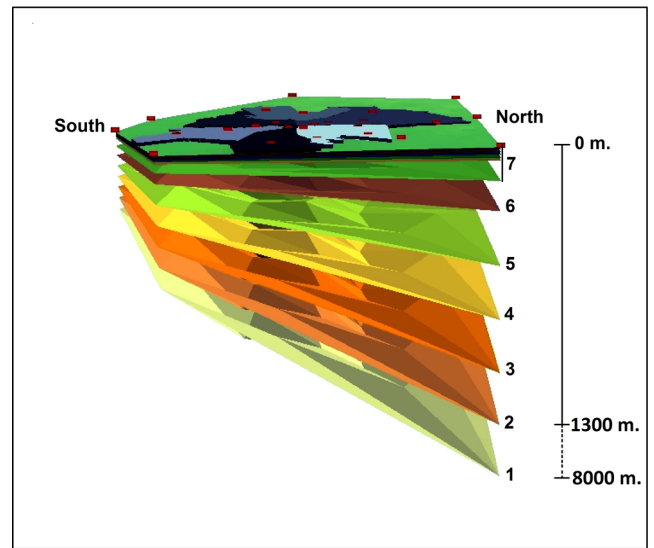


Figure 19. The resulted 3-D structure under Bucharest. The following matches with the geological interfaces are proposed: 1, Base of the sedimentary stack – early Devonian; 2, Interface Tertiary/Cretaceous; 6, Base of Palaeogene; 7, Quaternary layers – Holocene + Pleistocene.

Cretaceous (Mesozoic) and Tertiary geological units, which spatial distribution confirms that the bedrock is dipping from the south (500 m depth) to the north (about 1400 m depth). A second peak in the H/V ratios, poorly defined between 0.6 and 0.9 Hz using ambient vibration, becomes dominant in case of large Vrancea intermediate-depth earthquakes (Grecu *et al.* 2003). Its origin is interpreted as the interface between Quaternary and Neogene. The nature of this peak is complex and could be explained by the combination of the second higher mode of Rayleigh waves and SH waves contribution to the H/V ratios.

Due to the size of the URS array, a good approximation of the deep velocity structure under the city was achieved using the three-component frequency–wavenumber analysis of ambient

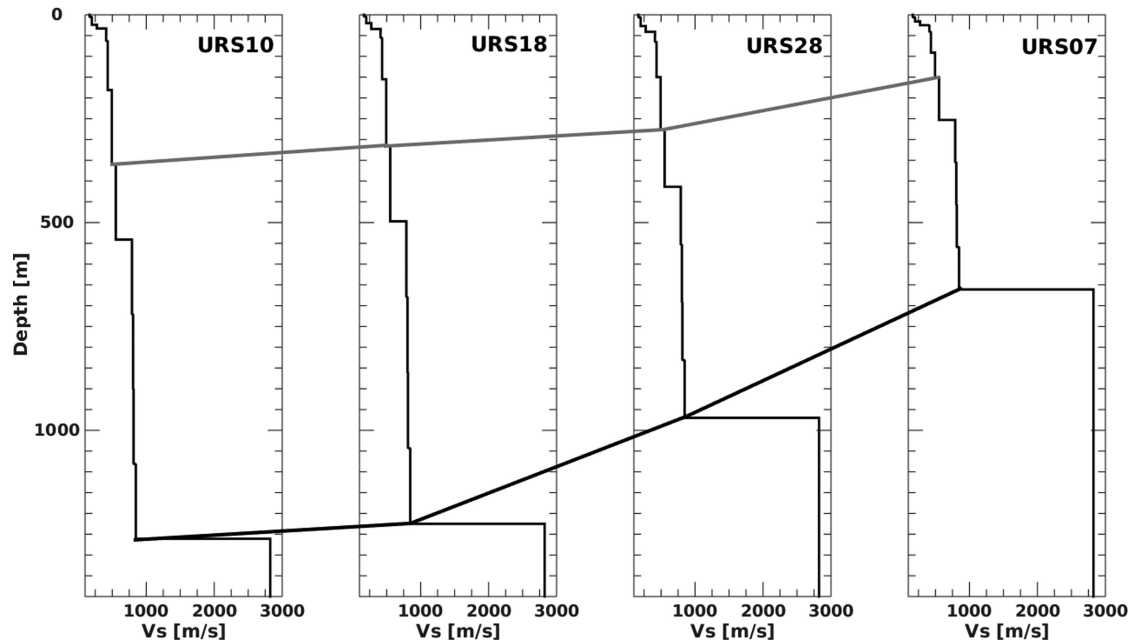


Figure 20. North-south cross-section (URS10, URS18, URS28 and URS07). The Quaternary layers are above the grey line, the five layers that are attributed to Miocene and Pliocene are between the two lines and the Cretaceous bed is below the black line.

vibrations. Using this method, we retrieved the dispersion curves for the fundamental, the second and third higher modes of Rayleigh waves. The dispersion curves for the fundamental and the first higher modes of Love waves were computed. The comparison with the Love dispersion curves proposed by Sèbe *et al.* (2009) shows a good match. The back-analysis showed that the fundamental and first higher modes are presenting two mode oscillations making the interpretation of the FK analysis difficult at first.

A joint inversion was performed successfully using the surface wave dispersion curves, their ellipticity and the fundamental resonance frequency of the site. The superficial structural model (depth <300 m) is constrained by existing borehole data. Our velocity profiles agree with the ones obtained from refraction by Hauser *et al.* (2001) and Raileanu *et al.* (2005) and are locally constrained by the geological data from BIGSEES project (Marmureanu, BIGSEES yearly report 2013). Our results are therefore bridging the gap between shallow and deep data. The variability of the Cretaceous bedrock over the entire city was retrieved and is fitting with the ones from drilling and geological studies proposed by Mandrescu *et al.* (2007). Also, using the entire dispersion curves and constraining the velocity ranges of the crystalline basement from refraction data (Hauser *et al.* 2001 and Raileanu *et al.* 2005), a velocity model with total depth of 8 km was built down to the Mesozoic/Paleozoic interface.

A relation between depth and frequency was derived allowing to estimate the Cretaceous bedrock depth in those areas for which a measurement of fundamental frequency of resonance of the S -wave (f_0^{SH}) is available. This relationship corresponds to an average shear wave velocity of the sediments of 747 m s^{-1} and can be used for the mapping of sedimentary basin bedrock of a large area of the Moesian Platform (approximately 600 km length and 400 km width) where a large number of single-station measurements were done.

Based on these data, a 3-D velocity model is proposed until the early Devonian layer for Bucharest area. This model will be used for ground-motion numerical modelling and will be implemented as a local model for Bucharest in Shakemap. At the same time,

the model will allow future studies focusing on the characterization and interpretation of the wavefield and on numerical 3-D wave-propagation modelling for hazard assessment.

ACKNOWLEDGEMENTS

This study was made in the framework of Sciex-NMS ch Programme (www.sciex.ch), No. 13.123, BIGSEES Project: ‘BrInging the Gap between Seismology and Earthquake Engineering: from the Seismicity of Romania towards a refined implementation of seismic action EN1998-1 in earthquake resistant design of buildings’ 72/2012 and PhD’s project of EFM. We thank to Dr Thomas Forbriger, from Geophysikalisches Institut, Karlsruher Institut für Technologie (KIT), Germany, for providing us the dispersion curves obtained by Sèbe *et al.* (2009) and to Dr Carmen Cioflan, from National Institute of Earth Physics, Romania, for the geological profiles used in her publications. We are grateful to the Editor, Dr Eiichi Fukuyama, and to the anonymous reviewers for their remarks and valuable suggestions, which helped us to improve the quality of this paper. The software suites Geopsy (www.geopsy.org, last accessed 01.07.2015) and ArcGis (www.esri.com/software/arcgis, last accessed 01.10.2015) have been used for this study.

REFERENCES

- Bala, A., 2014. Quantitative modelling of seismic site amplification in an earthquake-endangered capital city: Bucharest, Romania, *Nat. Hazards*, **72**, 1429–1445.
- Bala, A., Cristea, P., Raileanu, V. & Nitica, C., 2008. Continuous distribution of elastic parameters of the shallow quaternary layers along the 3C seismic profile east Bucharest, *Rom. Rep. Phys.*, **60**(1), 111–129.
- Bala, A., Grecu, B., Ciugudean, V. & Raileanu, V., 2009. Dynamic properties of the Quaternary sedimentary rocks and their influence on seismic site effects. Case study in Bucharest City, Romania, *Soil Dyn. Earthq. Eng.*, **29**, 144–154.
- Bonjer, K.-P., Oncescu, M.C., Driad, L. & Rizescu, M., 1999. A note on empirical site responses in Bucharest, Romania, in *Vrancea Earthquakes:*

- Tectonics, Hazard and Risk Mitigation*, pp. 149–162, eds Wenzel, F., Lungu, D. & Novak, O., Kluwer Academic Publishers.
- Bonnefoy-Claudet, S., Cornou, C., Bard, P.-Y., Cotton, F. & Kristek, J., 2006a. H/V ratio: a tool for site effect evaluation. Results from 1D noise simulations, *Geophys. J. Int.*, **167**, 827–837.
- Bonnefoy-Claudet, S., Cotton, F. & Bard, P.-Y., 2006b. The nature of noise wavefield and its applications for site effects studies, *Earth-Sci. Rev.*, **79**(3/4), 205–227.
- Capon, J., 1969. High-resolution frequency-wavenumber spectrum analysis, *Proc. IEEE*, **57**(8), 1408–1418.
- Cioflan, C.O., 2006. Seismic local effects, *PhD thesis*, University of Bucharest, Doctoral School of Physics, published in Romanian language. Ed. Universitatii ‘Alexandru Ioan Cuza’, Iasi.
- Cioflan, C.O., Apostol, B.F., Moldoveanu, C.L., Panza, G.F. & Marmureanu, G., 2004. Deterministic approach for the seismic microzonation of Bucharest, *Pure appl. Geophys.*, **161**, 1149–1164.
- Cioflan, C.O., Romanelli, F., Grecu, B., Popa, M., Măndrescu, N., Răileanu, V., Bălă, A. & Panza, G.F., 2007. General mapping of the strong ground motion in Bucharest area and related hazard/risk scenarios, in *Impact of Vrancea Earthquakes on the Security of Bucharest and other Adjacent Areas*, pp. 93–99, eds Panza, G.F., Radulian, M. & Kuznetsov, I., Independent Film.
- Cioflan, C.O., Marmureanu, A. & Marmureanu, G., 2009. Nonlinearity in seismic site effects evaluation, *Rom. J. Phys.*, **54**, 951–964.
- Ciugudean-Toma, V. & Stefanescu, I., 2006. Engineering geology of the Bucharest city area, Romania, in *IAEG -2006, Engineering Geology for Tomorrow's Cities*, Paper no. 235, pp. 1–8.
- Fäh, D., Kind, F. & Giardini, D., 2001. A theoretical investigation of average H/V ratios, *Geophys. J. Int.*, **145**, 535–549.
- Fäh, D., Kind, F. & Giardini, D., 2003. Inversion of local S-wave velocity structures from average H/V ratios, and their use for the estimation of site-effects, *J. Seismol.*, **7**, 449–467.
- Fäh, D., Stamm, G. & Havenith, H.B., 2008. Analysis of three-component ambient vibration array measurements, *Geophys. J. Int.*, **172**, 199–213.
- Grecu, B., Popa, M. & Radulian, M., 2003. Seismic ground motion characteristics in the Bucharest area: sedimentary cover versus seismic source control, *Rom. Rep. Phys.*, **55**(3), 322–331.
- Grecu, B., Radulian, M., Mandrescu, N. & Panza, G.F., 2007. H/V spectral ratios technique application in the city of Bucharest: can we get rid of source effect?, *J. Seismol. Earthq. Eng.*, **9**(1–2), 1–4.
- Hauser, F., Raileanu, V., Fielitz, W., Bala, A., Prodehl, C., Polonic, G. & Schulze, A., 2001. VRANCEA99—the crustal structure beneath the southeastern Carpathians and the Moesian Platform from a seismic refraction, *Tectonophysics*, **340**(3–4), 233–256.
- Hobiger, M., Le Bihan, N., Cornou, C. & Bard, P.-Y., 2012. Multicomponent Signal Processing for Rayleigh Wave Ellipticity Estimation Application to Seismic Hazard Assessment, *IEEE Signal Process. Mag.*, **29**(3), 29–39.
- Kienzle, A., Hannich, D., Wirth, W., Ehret, D., Rohn, J., Ciugudean, V. & Czurda, K., 2006. A GIS-based study of earthquake hazard as a tool for the microzonation of Bucharest, *Eng. Geol.*, **87**, 13–32.
- Konno, K. & Ohmachi, T., 1998. Ground-motion characteristics estimated from spectral ratio between horizontal and vertical components of microtremor, *Bull. seism. Soc. Am.*, **88**(1), 228–241.
- Lachet, C. & Bard, P.-Y., 1994. Numerical and Theoretical Investigations on the Possibilities and Limitations of Nakamura's Technique, *J. Phys. Earth*, **42**, 377–397.
- Liteanu, G., 1951. *Geology of the City of Bucharest*, Technical Studies, Serie E, Hydrogeology 1 (in Romanian).
- Lungu, D., Aldea, A., Moldoveanu, T. & Ciugudean, V., 1999. Near-surface geology and dynamic properties of soil layers in Bucharest, in *Vrancea Earthquakes: Tectonics, Hazard and Risk Mitigation*, pp. 137–148, eds Wenzel, F., Lungu, D. & Novak, O., Kluwer Academic.
- Mandrescu, N., Radulian, M. & Marmureanu, G., 2004. Site conditions and predominant period of seismic motion in the Bucharest urban area, *Rev. Roum. Geophys.*, **48**, 37–48.
- Mandrescu, N., Radulian, M. & Marmureanu, G., 2007. Geological, geophysical and seismological criteria for local response evaluation in Bucharest urban area, *Soil Dyn. Earthq. Eng.*, **27**, 367–393.
- Mandrescu, N., Radulian, M., Marmureanu, G. & Ionescu, C., 2008. *Integrate Research of the Geological, Geophysical and Seismological Data for Local Response Evaluation in Bucharest Urban Area*, Romanian Academy Publishing House.
- Marmureanu, G., 2013. Geological Database GDB for Romania, BIGSEES yearly report.
- Marmureanu, G., Androne, N., Radulian, M., Popescu, E., Cioflan, C.O., Placinta, A.O., Moldovan, I.A. & Serban, V., 2006. Attenuation of the peak ground motion for the special case of Vrancea intermediate-depth earthquakes and seismic hazard assessment at NPP Cernavoda, *Acta Geod. Geophys. Hung.*, **41**, 433–440.
- Marmureanu, G., Cioflan, C.O. & Marmureanu, A., 2010. *Seismic Local Hazard Research (Microzonation) of Bucharest Metropolitan Area*, Tehnopress.
- Michel, C., Edwards, B., Poggi, V., Burjáněk, J., Roten, D., Cauzzi, C. & Fäh, D., 2014. Assessment of Site Effects in Alpine Regions through Systematic Site Characterization of Seismic Stations, *Bull. seism. Soc. Am.*, **104**(6), 2809–2826.
- Moldoveanu, C.L., Radulian, M., Marmureanu, G. & Panza, G.F., 2004. Microzonation of Bucharest: State-of-the-Art, *Pure appl. Geophys.*, **161**, 1125–1147.
- Nakamura, Y., 1989. A method for dynamic characteristics estimation of subsurface using microtremor on the ground surface, *Rep. Railw. Tech. Res. Inst.*, **30**(1), 25–33.
- Nogoshi, M. & Igarashi, T., 1971. On the amplitude characteristics of microtremors, Part 2 (In Japanese with English abstract), *J. Seismol. Soc. Japan*, **24**, 26–40.
- Parolai, S., Richwalski, S.M., Milkereit, C. & Bormann, P., 2004. Assessment of the stability of H/V spectral ratios from ambient noise and comparison with earthquake data in the Cologne area (Germany), *Tectonophysics*, **390**(2004), 57–73.
- Poggi, V. & Fäh, D., 2010. Estimating Rayleigh wave particle motion from three-component array analysis of ambient vibrations, *Geophys. J. Int.*, **180**, 251–267.
- Poggi, V., Fäh, D., Burjáněk, J. & Giardini, D., 2012. The use of Rayleigh-wave ellipticity for site-specific hazard assessment and microzonation: application to the city of Lucerne, Switzerland, *Geophys. J. Int.*, **188**, 1154–1172.
- Radulian, M., Vaccari, F., Mandrescu, N., Panza, G.F. & Moldoveanu, C.L., 2000. Seismic hazard of Romania: deterministic approach, *Pure appl. Geophys.*, **157**, 221–247.
- Raileanu, V., Bala, A., Hauser, F., Prodehl, C. & Fielitz, W., 2005. Crustal properties from S-wave and gravity data along a seismic refraction profile in Romania, *Tectonophysics*, **410**, 251–272.
- Ritter, J.R., Balan, S., Bonjer, K., Diehl, T., Forbriger, T., Marmureanu, G., Wenzel, F. & Wirth, W., 2005. Broadband urban seismology in the Bucharest metropolitan area, *Seismol. Res. Lett.*, **76**(5), 574–580.
- Sambridge, M., 1999. Geophysical inversion with a neighborhood algorithm I. Searching a parameter space, *Geophys. J. Int.*, **138**, 479–494.
- Satoh, T., Kawase, H. & Matsushima, S.I., 2001. Differences between site characteristics obtained from microtremors, S-waves, P-waves, and codas, *Bull. seism. Soc. Am.*, **91**, 313–334.
- Sèbe, O., Forbriger, T. & Ritter, J.R., 2009. The shear wave velocity underneath Bucharest city, Romania, from the analysis of Love waves, *Geophys. J. Int.*, **176**, 965–979.
- Wathelet, M., 2008. An improved neighborhood algorithm: parameter conditions and dynamic scaling, *Geophys. Res. Lett.*, **35**(May), 1–5.
- Wathelet, M., Jongmans, D. & Ohrnberger, M., 2004. Surface-wave inversion using a direct search algorithm and its application to ambient vibration measurements, *Near Surf. Geophys.*, **2**, 211–221.
- Wathelet, M., Jongmans, D., Ohrnberger, M. & Bonnefoy-Claudet, S., 2008. Array performances for ambient vibrations on a shallow structure and consequences over Vs inversion, *J. Seismol.*, **12**, 1–19.
- Zaharia, B., Radulian, M., Popa, M., Grecu, B., Bala, A. & Tataru, D., 2008. Estimation of the local response using Nakamura method for Bucharest area, *Rom. Rep. Phys.*, **60**(1), 125–134.